Supporting Information

Imaging of HNO anti-inflammatory effects via a Near-Infrared Fluorescent Probe in Cell and in Rat Gouty Arthritis Models

Yan Huang,[a,b] Xia Zhang,[b,d] Na He,[b,] Yue Wang, [b,d] Qi Kang,[a]* Dazhong Shen,[a] Fabiao Yu,[b,c]* and Lingxin Chen[b,e]*

[a] College of Chemistry, Chemical Engineering and Materials Science, Key Laboratory of Molecular and Nano Probes, Ministry of Education, Shandong Normal University, Jinan 250014, China
[b] Key Laboratory of Coastal Environmental Processes and Ecological Remediation, The Research Center for Coastal Environmental Engineering and Technology, Yantai Institute of Coastal Zone Research, Chinese Academy of Sciences, Yantai 264003, China
[c] Institute of Functional Materials and Molecular Imaging, College of Emergency and Trauma, Hainan Medical University, Haikou 571199, China
[d] University of Chinese Academy of Sciences, Beijing 100049, China
[e] College of Chemistry and Chemical Engineering, Qufu Normal University, Qufu 273165, China

*E-mails: kangqi@sdnu.edu.cn (Q. Kang); fbyu@yic.ac.cn (F. Yu); lxchen@yic.ac.cn (L. Chen)

List of Contents

1. General Experimental Section

Instruments. Mice imaging was performed on in vivo FX PRO (Bruker) system and Perkinelmer IVIS Lumina XRMS Series III In Vivo Imaging System. Fluorescence spectra were obtained by Shimadzu RF-5301PC Spectrofluorometer with a Xenon lamp and 1.0-cm quartz cells. Absorption spectra were measured on TU-1810DSPC UV-visible spectrophotometer (Beijing Persee). Mass spectra were taken on LCQ Fleet LC-MS System (Thermo Fisher Scientific). ^{1}H NMR, ^{13}C NMR and ^{31}P NMR spectra were recorded on a Bruker spectrometer. MTT Assay was carried out by a microplate reader (Tecan, Austria). The fluorescence images of cells were taken using a confocal laser scanning microscope (Japan Olympus Co., Ltd) with an objective lens (×60). Intracellular fluorescence detection was carried out on flow cytometry (Aria, BD) with excitation at 633 nm and emission at 750-810 nm.

Materials. The purity of **Mito-JN** was separated on a Shimadzu LC-20AT HPLC system equipped with fluorescence and UV-vis absorption detectors. When it was used for imaging, the purity of **Mito-JN** was greater than 95%. HEPES was obtained from Aladdin and 3-(4,5-Dimethylthiazol-2-yl)-2,5-diphenyltetrazolium bromide (MTT) was purchased from Sigma-Aldrich. Raw 264.7 Murine Macrophages (RAW264.7 cells), human astrocytoma cells (U87 cells) and human cervical carcinoma cells (HeLa cells) were obtained from the Committee on Type Culture Collection of the Chinese Academy of Sciences. Phosphorylated NF-κB p65 and NF-κB p65, phosphorylated p38 and p38 were obtained from Cell Signaling Technology (Beverly, MA. USA).

Cell Cultures. Mouse macrophages cells (RAW264.7 cells), human astrocytoma cells (U87 cells) and BV-2 microglial cell line (BV-2 cells) were obtained from the Committee on Type Culture Collection of the Chinese Academy of Sciences. RAW264.7 cells, U87 cells and BV-2 cells were cultured in Dulbecco's Modified Eagle Medium (DMEM) supplemented with 10% FBS (fetal bovine serum) in an atmosphere of 5% CO_2 and 95% air at 37 °C.

Preparation of analytes. **Mito-JN** (1 mM) and Cy-Mito (1 mM) were prepared in DMSO and stored at 4°C in darkness. Angeli's salt (AS) was prepared as reported by King and Nagasawa and stored dry at -20°C in a refrigerator.[1] S-nitrosoglutathione (GSNO) was synthesized from GSH, according to the published procedure.[2] Peroxynitrite ($ONOO^-$) solution was synthesized as reported.[3] NO was generated in form of 3-(Aminopropyl)-1-hydroxy-3-isopropyl-2-oxo-1-triazene (NOC-5, 100 μM/ml).[4] NO_2^- was generated from $NaNO_2$. O_2^- was created by the enzymatic reaction of xanthine/xanthineoxidase (XA/XO; 6.0 μM/3 mU) at 25 °C for 5 min.[5] Methyl linoleate (MeLH) and 2,2'-azobis-(2,4-dimethyl) valeronitrile (AMVN) were used to produce MeLOOH.[6] ClO^- was generated from NaClO. All other reagents and chemicals were all from commercial sources and used without further purification. Water used in all experiments was doubly distilled and purified by a Milli-Q system (Millipore, Bedford, MA, USA).

Spectroscopic Methods. UV-visible spectra were obtained with 1.0-cm glass cells. The probe **Mito-JN** (DMSO, 20 μL, 2 μM) was added to a 10.0-mL color comparison tube, and diluted to 2 μM with HEPES buffer (10 mM, 0.5% DMSO, 0.5% TW 80, pH 7.4). **Mito-1** and phosphine oxide were also performed as above. Fluorescence spectra were obtained with a Xenon lamp and 1.0-cm quartz cells. The probe (DMSO, 10 μL, 2 μM)

was added to a 5.0-mL color comparison tube. After diluted to 2 μM with HEPES buffer (10 mM, 0.5% DMSO, 0.5% TW 80, pH 7.4), different concentrations of AS were added. The mixture was incubated for 20 min before measurement. Then the fluorescence emission spectra were integrated from 670 to 750 nm with excitation at 694 nm.

Cell Staining Procedures and Colocalization-imaging Experiments. The cells were plated on 6-well plates and allowed to adhere at 37 °C, 5% CO_2, 24 h before imaging. The culture medium was then removed, and the cells were washed once with 1 mL of Dulbecco's Modified Eagle Medium (DMEM). RAW264.7 cells were placed in 1 mL of DMEM and loaded with 2 μM Hoechst 33342 for 30 min before staining with 1 μM **Mito-JN** for 20 min. After washing the cells three times with DMEM to remove the excess probe, the cells were placed in 1 mL of DMEM and treated with 1 mM NOC-5 and 100 μM NaHS for 20 min. Finally, 1 μg/mL MitoTracker Green FM was added and the cells were incubated for another 15 min at 37°C. Finally, the cells were rinsed with DMEM three times and mounted on the microscope. Fluorescent images were acquired on an Olympus Fluo View FV1000 confocal laser-scanning microscope (Japan) with an objective lens (×60). The spectrally separated images acquired from the three dyes were estimated using Image-Pro Plus software.

Flow cytometry. FCM assay was carried out for the detection of the intramolecular generation of HNO with probe **Mito-JN**. The cells were cultured at 2.0×10^5 cells/well in 6-well plates, and treated with 1 μM **Mito-JN** for 20 min, and then the cells were further incubated with different concentration of AS for 20 min at 37 °C. After harvest, cells were washed, and resuspended in PBS and analyzed by flow cytometry.

Cytotoxicity of Mito-JN. The cytotoxicity of probe **Mito-JN** was assessed by the MTT assay. RAW264.7 cells were seeded into 96-well cell culture plate at a final density of 8×10^3 cells/well. And then different concentrations of **Mito-JN** (0.1 μM, 1 μM, 10 μM, 100 μM) were added to the wells. The cells were then incubated for 24 h at 37 °C under 5% CO_2. Subsequently, MTT was added to each well (final concentration 5 mg/mL) for an additional 4 h at 37 °C under 5% CO_2, then formazan crystals which were dissolved in 150 μL DMSO formed. The amount of MTT formazan was qualified by the absorbance (OD) at 570 nm using a microplate reader (Tecan, Austria). Calculation of IC_{50} values were done according to Huber and Koella. The results are the mean standard deviation of six separate measurements.

Establish Inflammatory Cell Model by LPS. U87 cells were cultured in DMEM supplemented with 10% FBS (fetal bovine serum) in an atmosphere of 5% CO_2 and 95% air at 37 °C. 1 μg/mL lipopolysaccharide (LPS) was added to HeLa cells exposure for 24h.

Mice Imaging. Six to eight-week-old BALB/c mice were obtained from Binzhou Medical University. Mice were group-housed on a 12:12 light-dark cycle at 22 °C with free access to food and water. BALB/c mice, 20-25 g, were selected and divided into different groups. Mice were anesthetized prior to injection and during imaging via inhalation of isoflurane. All the BALB/c mice were selected and divided into two groups. BALB/c mice (20-25 g) were given intraperitoneal (i.p.) injections of **Mito-JN** (50 μM, 50 μL in 1:9 DMSO/ saline v/v), then mice in group A was intraperitoneally injected with AS (500 μM, 50 μL in saline) for 20 min. Finally, two groups of mice were anesthetized by i.p. injections of 4% chloral hydrate (0.25 ml). Then two groups of mice were imaged by using a FX PRO in vivo imaging system, with an excitation filter of 680 nm and an emission of 690-750 nm. The results were the mean standard deviation of five separate measurements. Additionally, we merged the fluorescence image with the corresponding X-ray image to clearly display the reaction site of the mice. All experimental procedures were conducted in conformity with institutional guidelines for the care and use of laboratory animals, and protocols were approved by the Institutional Animal Care and Use Committee in Binzhou Medical University, Yantai, China.

Western blot analysis: All the rat gouty arthritis models for imaging were continuous reared on a 12:12 light-dark cycle at 22 °C with free access to food and water for 2 days. Then the synovial membrane tissue samples of ankle joint were stripped and washed for three times before lysis of tissue. Protein extracts were prepared by suspending the tissue in 200 μL RIPA lysis buffer containing 1% PMSF (Solarbio, China) and 20% PhosSTOP (Roche, Germany). Then the extracts were quantified with BCA protein assay kit (Biogot, China). After denatured, the equal amounts of protein were electrophoresed on 10% SDS-polyacrylamide gels (Bio-Rad, USA) and transferred to PVDF membranes. The membrane was incubated with 5% BSA (Sigma-Aldrich, USA) and incubated with primary antibodies overnight at 4 °C with gentle shake. A horseradish peroxidase (HRP)-conjugated secondary antibody (Cell Signaling Technology, USA) was used to mirror the quantity of proteins and signals were detected with an enhanced chemiluminescence (ECL) detection system. The results were analyzed by ImageJ to acquire the grey value of every bond.

H&E staining: Synovial membrane tissue of ankle joint from normal rats and gouty arthritis rats were excised and fixed in 10% formaldehyde and embedded in paraffin. Then the treated synovial membrane tissue of ankle joint were prepared to frozen sections and stained with hematoxylin and eosin (H&E) to confirm histology.

2. Synthesis of Fluorophore

Scheme S1. Synthesis of **Mito-JN**

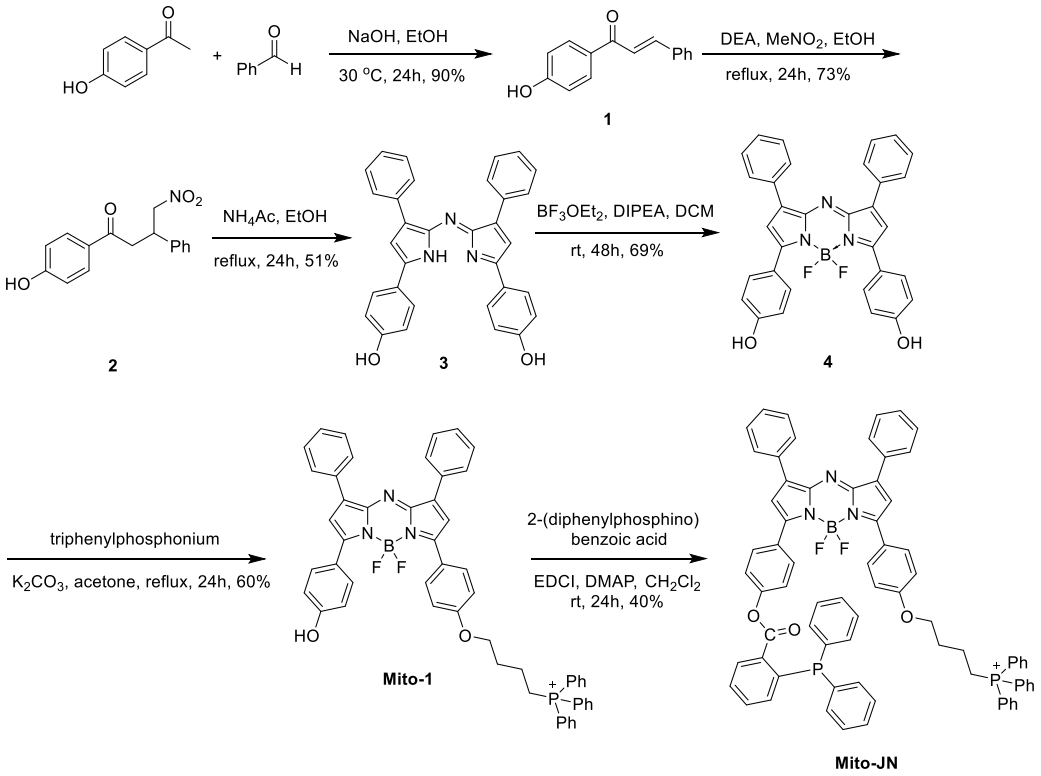

Synthesis of 1: 4'-Hydroxyacetophenone (13.6 g,100 mmol) in ethanol (140 mL) was added to the solution of sodium hydroxide (8.4 g, 210 mmol) in 60 mL water under ice bath，then benzaldehyde（10.13 mL, 100 mmol）diluted with ethanol (140 mL) was dropwised to the cold solution. The resulting solution was stirred at room temperature for 15 h, and then the HCl was added to the solution. Finally, the solution was cold in ice water, filtered, and crystallized with ethanol to yield light yellow crystal chalcone **1** (20.16 g, 90%), m.p.180-182 ºC. ^{1}H NMR (500 MHz, $CDCl_3$-D_1) δ (ppm): 10.41 (s, 1H), 8.08-8.05 (m, 2H), 7.92-7.85 (m, 3H), 7.69-7.66 (m, 1H), 7.47-7.43 (m, 3H), 6.91-6.88 (m, 2H). LC-MS (ESI$^+$): m/z $C_{15}H_{12}O_2$ calcd. 224.0837, found [M-H]$^-$ 223.0758.

Synthesis of 2: A solution of chalcone **1** (2.02 g, 9 mmol) in EtOH (15 mL) was treated with diethylamine (4.6 mL, 45 mmol) and nitromethane (4.8 mL, 90 mmol), then heated under reflux for 24 h. The solution was cooled and then neutralized with HCl, partitioned between EtOAc and H_2O (1:1). The organic layer was separated, dried over sodium sulfate and evaporated. The residue was stirred in cold Et_2O for 10 min and filtered to give the product as yellowish crystalline compound 2 (1.87 g, 73%), m.p. 112-113 ºC. ^{1}H NMR (500 MHz, DMSO-D_6) δ (ppm): 10.20 (s, 1H), 7.77 (d, 2H), 7.28-7.20 (m, 5H), 6.78 (m, 2H), 4.86 (m, 2H), 3.93 (m, 1H), 3.81 (m, 2H). LC-MS (ESI$^+$): m/z $C_{16}H_{15}NO_4$ calcd. 285.1001, found [M-H]$^-$ 284.0928.

Synthesis of 3: Compound 2 (2.0 g, 7.0 mmol) and ammonium acetate (18.9 g, 245 mmol) in EtOH (50 mL) were heated under reflux for 24 h. The reaction was cooled to room temperature. Then, the product was spin steamed and extracted in EtOAc and H_2O (1:1).The organic layer was evaporated to dry and yielded **3** as blue-black solid (1.72 g, 51%), mp 245-246 °C. ^{1}H NMR (500 MHz, DMSO-D_6) δ (ppm): 10.26-10.21 (s, 2H), 7.53-7.24 (m, 13H), 7.10-7.07 (m, 3H), 6.49-6.47 (d, 4H), 5.26 (s, 1H). LC-MS (ESI$^+$): m/z $C_{32}H_{23}N_3O_2$ calcd. 481.1790, found [M-H]$^-$ 480.1717.

Synthesis of 4: Compound 3 (0.15 g, 0.31 mmol) was dissolved in anhydrous CH_2Cl_2, treated with diisopropylethylamine (0.54 mL, 3.11 mmol) and BF_3diethyletherate (0.55 mL, 4.35 mmol), and stirred under argon for 48 h. The colour of solution changed from blue to green. The course of the reaction is confirmed by thin-layer chromatography (TLC).The product was extracted in CH_2Cl_2/H_2O (1:1), and the organic layer evaporated to dryness, and then purified by column chromatography on silica eluting with CH_2Cl_2/EtOAc (4:1) gave the Aza-BODIPY as atropurpureus solid (0.11 g, 69%), m.p 253-254 °C. ^{1}H NMR (500 MHz, DMSO-D_6) δ (ppm): 10.46 (s, 2H), 8.16-7.80 (m, 8H), 7.56-7.48 (m, 6H), 7.48-7.45 (m, 2H), 6.96-6.94 (4H). LC-MS (ESI^+): m/z $C_{32}H_{22}BF_2N_3O_2$ calcd. 529.1773, found $[M-H]^-$ 528.1702.

Synthesis of Mito-1. Aza-BODIPY fluorophore (Compound **1**) was synthesized starting from 4-hydroxychalcone following a previously reported protocol (Scheme S1, ESI†).[47] Compound **1** (52.9 mg，0.1 mmol) and (4-Bromobutyl) triphenylphosphonium bromide（47.8mg，0.1 mmol）were dissolved in dry acetone (25 mL), then anhydrous potassium carbonate (27.5 mg，0.2 mmol) was added. The mixture was stirred under a dry argon atmosphere for 24 h and monitored by TLC. After the reaction was finished, the mixture was cooled to room temperature, evaporated under reduced pressure and partitioned with CH_2Cl_2 and saturated NaBr solution. Finally, the organic layer was separated. Purification by column chromatography on silica eluting with EtOAc/CH_3OH (3:1) gave the product **Mito-1** as dark green crystals (33.84 mg, 40%). ^{1}H NMR (500 MHz, DMSO-*d_6*) δ (ppm): 9.59 (s, 1H), 8.06-8.02 (m, 2H), 7.97-7.92 (m, 4H), 7.87-7.81 (m, 5H), 7.79-7.71 (m, 2H), 7.70-7.58 (m, 16H), 7.18-7.16 (d, 2H), 7.05 (s, 1H), 6.79 (s, 1H), 6.64-6.62 (d, 2H), 4.14-4.10 (t, 2H), 1.75-1.73 (m, 2H), 0.97-0.92 (m, 4H). ^{13}C NMR (125 MHz, $CDCl_3$-D) δ (ppm):172.16, 171.15, 150.00, 147.83, 135.21, 133.79, 133.71, 133.52, 133.44, 130.62, 130.52, 129.27, 129.08, 128.55, 128.45, 118.97, 118.01, 117.48, 116.65, 114.47, 60.39, 29.70, 21.05, 14.20. ES-MS: *m/z* $C_{54}H_{44}BF_2N_3O_2P^+$, calcd 846.32, $[M + H]^+$ 846.56.

Synthesis of Mito-JN: Mito-1 (84.6 mg, 0.1 mmol), 2-(diphenylphosphino) benzoic acid (30.6 mg, 0.1 mmol), 4-(dimethylamino) pyridine (12.2 mg, 0.1 mmol), and 1-ethyl 3-(3-dimethylaminopropyl) carbodiimide hydrochloride (9.6 mg, 0.05 mmol) were dissolved in dry CH_2Cl_2. The reaction mixture was stirred for 24 h at room temperature under a dry argon atmosphere, monitored by TLC. And then the mixture was poured into water and extracted with CH_2Cl_2. The organic layer was separated, washed with NaBr in saturated aqueous solution, and dried over Na_2SO_4. The solvent was evaporated, and the crude product of **Mito-JN** was purified by column chromatography over silica gel with EtOAc/CH_3OH (3:1) gave **Mito-JN** as dark green crystals (34.02 mg, 30%). ^{1}H NMR (500 MHz, $CDCl_3$-D) δ (ppm): 8.28-8.25 (m,1H), 8.07-8.00 (m, 3H), 7.72-7.20 (m, 43H), 7.10-7.07 (m, 1H), 6.94-6.91 (m, 1H), 4.32-4.29 (t, 2H), 1.75-1.69 (m, 2H), 1.46-1.42(m, 2H), 0.98-0.95(t, 2H). ^{13}C NMR (125 MHz, $CDCl_3$-D) δ (ppm): 167.72, 137.58, 137.49, 135.02, 135.00, 134.11, 133.94, 133.73, 133.66, 132.33, 132.07, 130.92, 130.53, 130.43, 129.41, 129.25, 128.84, 128.64, 128.59, 128.43, 121.74, 118.62, 118.25, 117.94, 114.90, 65.57, 30.58, 19.19, 13.73. ^{31}P NMR (200 MHz, $CDCl_3$-D) δ (ppm): 28.88. ES-MS: m/z $C_{73}H_{57}BF_2N_3O_3P^{2+}$, calcd 1134.3931, $[M]^+$ 1134.3931.

3. Effect of pH Values on Probe

As a starting point, it is necessary to understand the pH effect on the potential fluorescence behaviour of our probe **Mito-JN** in the absence and presence of HNO (HEPES buffer solution 10 mM, 0.5% DMSO, 0.5% TW 80).

Angeli's salt (AS) has been employed as HNO donor since HNO is not stable. The results demonstrate that fluorescence intensity of **Mito-JN** shows pH-dependent property over the pH range from 4.0-9.0 (Figure. S1, ESI†). After the probe was incubated with AS for 20 min, the fluorescence intensity increased dramatically and stayed at high level before pH 6.0, and then decreased gradually with the increase of pH values, which might be ascribed to the decreased decomposition rate of AS into HNO under base conditions. When pH ranges from 7.0 to 8.0, the fluorescence intensity of **Mito-JN** with AS is still 2-3 fold higher than that of only **Mito-JN**, which indicates that our probe **Mito-JN** would be suitable to be applied in mitochondria in which pH ranges from 7.0 to 8.0.

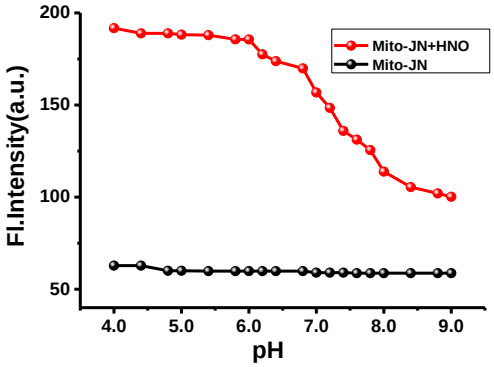

Figure S1. The effects of pH values on the fluorescence intensity (λ_{ex}= 694 nm, λ_{em}= 700 nm) of probe **Mito-JN** (2 μM) in the absence and presence of HNO (HEPES buffer solution 10 mM, 0.5% DMSO, 0.5% TW 80). pH values: 4.0, 4.4, 4.8, 5.0, 5.4, 5.8, 6.0, 6.2, 6.4, 6.8, 7.0, 7.2, 7.4, 7.6, 7.8, 8.0, 8.4, 8.8, 9.0, 10.0.

4. Effect of Tween 80 to Fluorescence Intensity

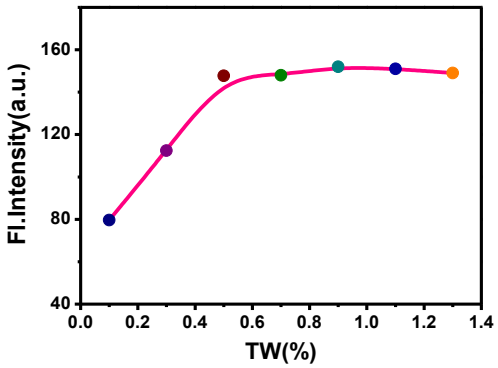

Figure S2. The effect of Tween 80 on the fluorescence intensity (λ_{ex}= 694 nm, λ_{em}= 700 nm) of **Mito-1** (2 μM) in HEPES (10 mM, 0.5% DMSO, pH 7.4).

5. Absorption Spectra of Mito-JN

The absorption and fluorescent spectra of **Mito-JN** were examined in HEPES buffer solution (10 mM, pH 7.4). **Mito-JN** exhibited an absorption maximum at 680 nm ($\varepsilon = 3.70 \times 10^4$ $M^{-1}cm^{-1}$) (Figure.S3). And the absorption maximum of **Mito-1** and phosphine oxide were observed at 704 nm ($\varepsilon = 3.25 \times 10^4$ $M^{-1}cm^{-1}$) and 684 nm ($\varepsilon = 3.05 \times 10^4$ $M^{-1}cm^{-1}$), respectively. The wavelength at 694 nm which was near isosbestic point was chosen as the excitation light.

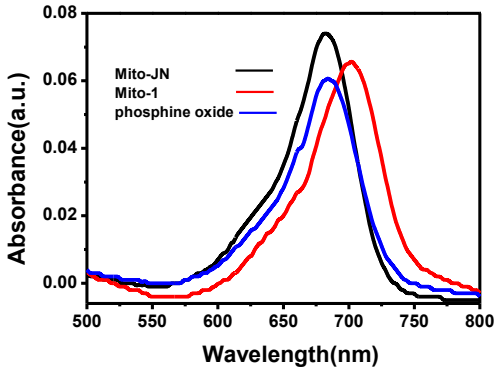

Figure S3. Absorption spectra of 2 μM **Mito-JN** (black) and two products: 2 μM **Mito-1** (red), 2 μM phosphine oxide (blue).

6. Determination of Quantum Yields

The fluorescence quantum yields of **Mito-1** and **Mito-JN** were determined according to the following expression: [7]

$$\varphi_u = \frac{(\varphi_s)(FA_u)(A_s)(\lambda_{exs})(\eta_u^2)}{(FA_s)(A_u)(\lambda_{exu})(\eta_s^2)}$$

Where φ is fluorescence quantum yield; the subscripts u and s refer to the unknown and the standard, respectively; F is integrated fluorescence intensity under the corrected emission spectra; A is the absorbance at the excitation wavelength; η is the refractive index of the solution. We chose Mg-tetra-*tert*-butylphthalocyanine as standard, which has a fluorescence quantum yield of 0.84 according to the literature.[8]

7. Selectivity of Probe for Common Metal Ion and Anions

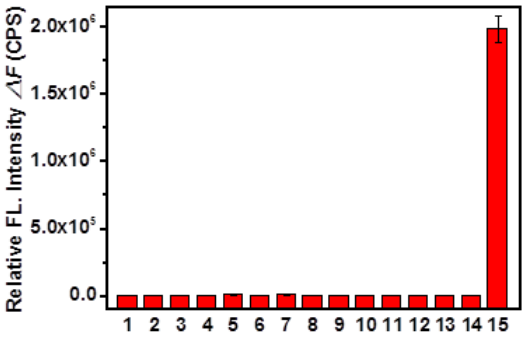

Figure S4. Fluorescence responses of Mito-JN to various metal ions and anions. Legend: 1, K^+ (1 mM); 2, Na^+ (1 mM); 3, Ca^{2+} (1 mM); 4, Mg^{2+} (1 mM); 5, Zn^{2+} (1 mM); 6, Cu^{2+} (1 mM); 7, Cl^- (1 mM); 8, Br^- (1 mM); 9, HSO_3^- (100 μM); 10, SO_4^{2-} (100 μM); 11, SO_3^{2-} (100 μM); 12, $S_2O_3^{2-}$ (100 μM); 13, CO_3^{2-} (100 μM); 14, $H_2PO_4^{2-}$ (100 μM); 15, AS (10 μM). Data were recorded in 10 mM HEPES buffer (pH=7.4, 10 mM) at 37 °C for 35 min. λ_{ex} = 694 nm, λ_{em} = 730 nm.

8. MTT Assay

The cytotoxicity of probe **Mito-JN** was assessed by the MTT assay. RAW264.7 cells were seeded into 96-well cell culture plate at a final density of 8×10^3 cells/well. And then different concentrations of **Mito-JN** (0.1 μM, 1

μM, 10 μM, 100 μM) were added to the wells. The cells were then incubated for 24 h at 37 °C under 5% CO_2. Subsequently, MTT was added to each well (final concentration 5 mg/mL) for an additional 4 h at 37 °C under 5% CO_2, then formazan crystals which were dissolved in 150 μL DMSO formed. The amount of MTT formazan was qualified by the absorbance (OD) at 570 nm using a microplate reader (Tecan, Austria). Calculation of IC_{50} values were done according to Huber and Koella. The results are the mean standard deviation of six separate measurements.

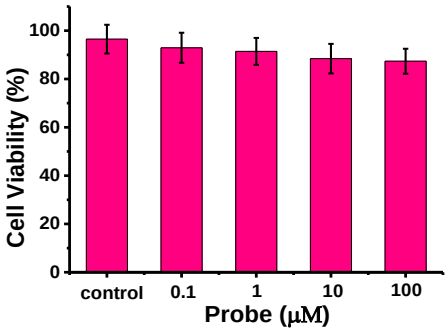

Figure S5. Effects of **Mito-JN** at varied concentrations on the viability of RAW264.7 cells.

9. The time-dependent assay of Mito-JN in living cells.

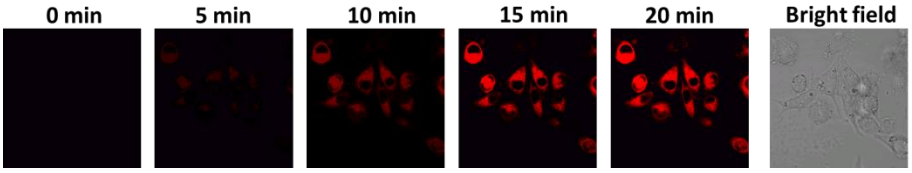

Figure S6. The time-dependent assay described the good photo-stability and strong fluorescence increase of **Mito-JN** (1 μM), the cells were treated with 1 mM NOC-5 and 100 μM NaHS.

10. Flow Cytometry Analysis of Mitochondrial Isolation.

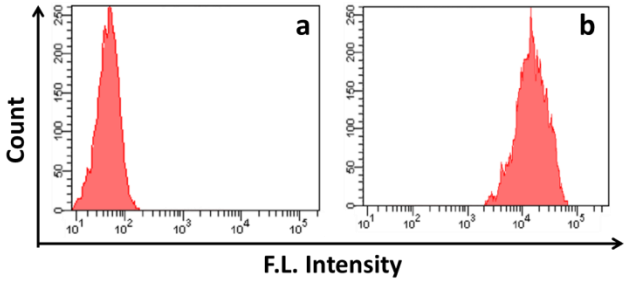

Figure S7. Mitochondrial flow cytometry analysis for the cells in Figure 1k. a) The cells were incubated under 37 °C for 15 min in 1 μM **Mito-JN** as control. b) The cells were incubated under 37 °C for 15 min in 1 μM **Mito-JN**. Then the cells were next treated with NOC-5 (1 mM) and NaHS (100 μM). After isolated mitochondria, flow cytometric analysis were performed: excitation wavelength was 680 nm. The collected wavelengths was 690 -720 nm.

11. The Interference of GSNO for Cell Imaging.

Firstly, RAW 264.7 cells were treated with Mito-JN for 20 min, then the cells were treated with 20 μM GSNO for 20 min. The cells were imaging by laser scanning confocal microscope. As shown as Figure S7, a much weaker

fluorescence image was obtained which compared with Figure 2b and 2c. These results confirmed that GSNO was almost no interference for cell imaging.

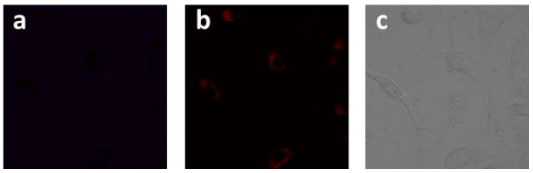

Figure S8. (a) RAW 264.7 cells were treated with Mito-JN for 20 min, (b) then the cells were treated with 20 μM GSNO for 20 min. (c) Bright-field images.

12. Bright-field Images of Figure 2

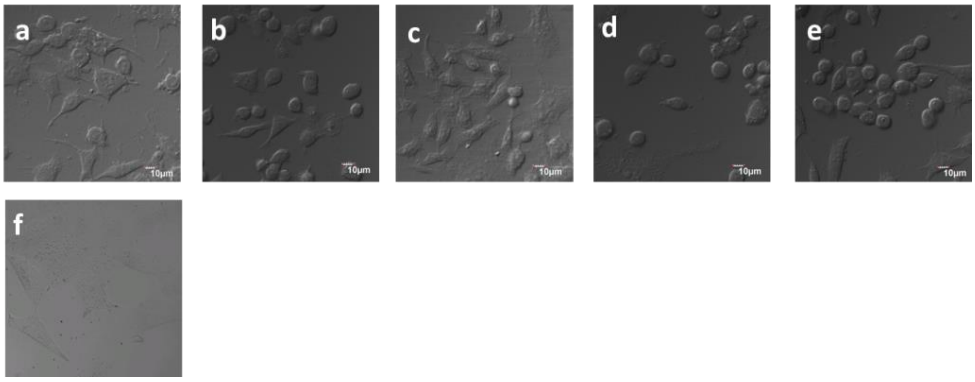

Figure S9. (a) - (e) Bright-field images of Figure 2a-2e. (f) Bright-field images of Figure 2k. Scale bar: 10 μm.

13. Additional generation of H_2S_n in NO/H_2S crosstalk.

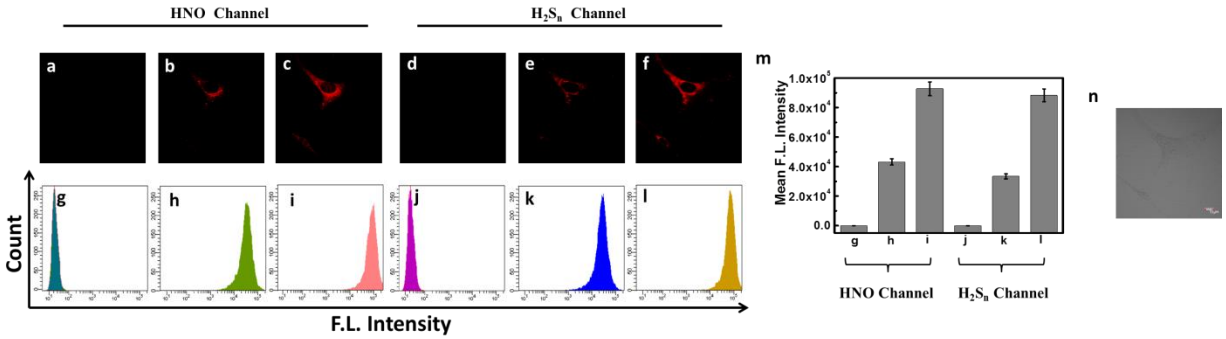

Figure S10. Fluorescence confocal microscopic images and flow cytometry assay of living U87 cells with **Mito-JN** and Cy-Mito. a), d) The cells were loaded with 1 μM **Mito-JN** and 1 μM Cy-Mito. b), e) As described in a, d, and then the cells were treated with 1 mM NOC-5 and 100 μM NaHS for 10 min. c), f) As described in b, e, and the images of 20 min later. g) – l) Flow cytometry assay of U87 cells correspond with a – f. m) Mean fluorescence intensity of parts g − l. n) Bright-field images. **Mito-JN** (red channel: λ_{ex} = 680 nm, λ_{em} = 690-720 nm). Cy-Mito (red channel: λ_{ex} = 730 nm, λ_{em} = 750-800 nm). Images are representative of n = 5 independent experiments. Scale bar = 10 μm.

14. Anti-inflammatory Effect of AS in Inflammatory Cell Model

The BV-2 microglial cells as the control group, BV-2 cells treated with LPS as the LPS group, BV-2 cells

treated with LPS and after treated with AS as the LPS+AS group. We utilized western blot analysis to analyze the expression of inflammation associated protein: phosphorylated p38 (P-p38), p38 MAPK (T-p38), phosphorylated NF-κB p65 (P-p65) and NF-κB p65 (T-p65). As shown as Figure S10, the P-p38 and P-p65 were activated in inflammation cells. As expected, the protein expressions of P-p38 and P-p65 were drastically reduced after the simultaneous addition of AS. This result was consistent with Figure 4 in manuscript. All these data demonstrated that HNO possessed anti-inflammatory effect in inflammatory cell model.

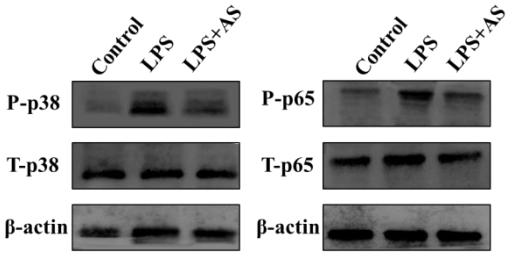

Figure S11. Western blotting analysis of P-p38, T-p38, P-p65 and T-p65 of BV-2 cells in different groups. β-actin was used as a loading control.

15. Bright-field Images of Figure 4

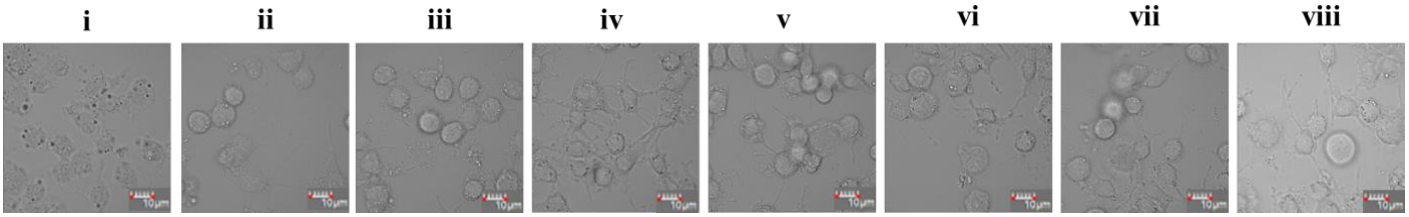

Figure S12. Bright-field images of Figure 4. Scale bar: 10 μm.

16. Bright-field Images of Figure 5

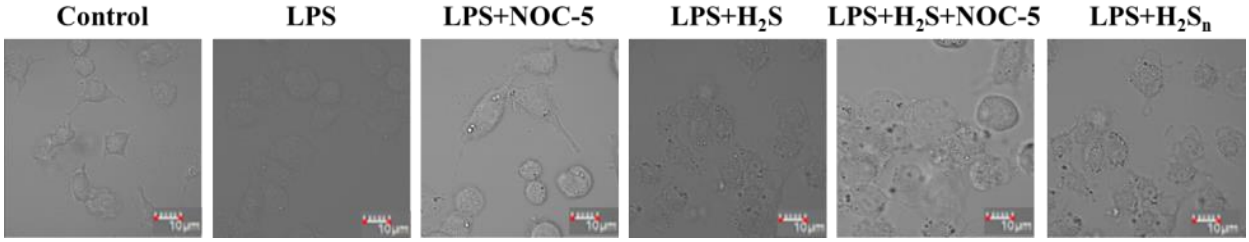

Figure S13. Bright-field images of Figure 5. Scale bar: 10 μm.

17. The average fluorescence intensity of Figure 5a

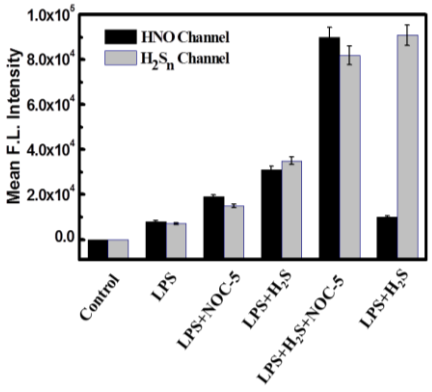

Figure S14. The average fluorescence intensity of Figure 5a. Data are presented as mean ± SD (n = 5).

18. The fluorescence intensity of Figure 7a

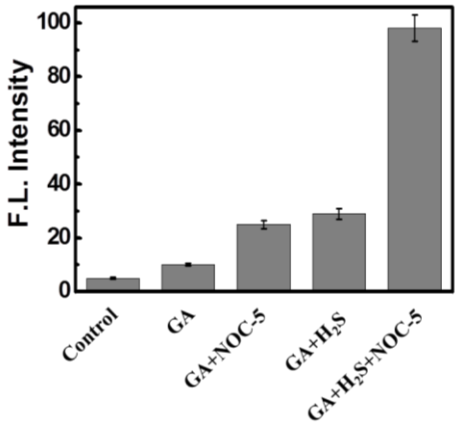

Figure S15. The fluorescence intensity of Figure 7a. Data are presented as mean ± SD (n = 5).

19. Western blot of GA group treated with H_2S_n.

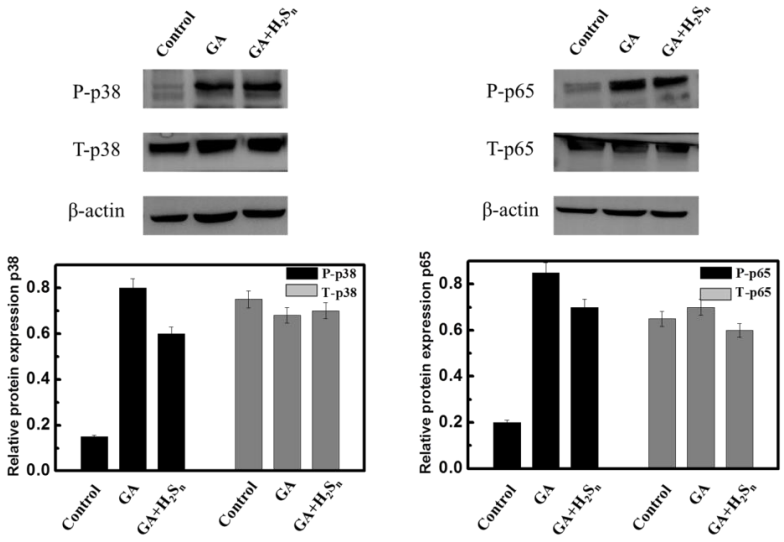

Figure S16. Western blotting analysis of P-p38, T-p38, P-p65 and T-p65 of three groups. Data are presented as mean ± SD (n = 5).

20. ^{1}H NMR, ^{13}C NMR and ^{31}P NMR of Mito-JN.

^{1}H NMR of **Mito-JN**

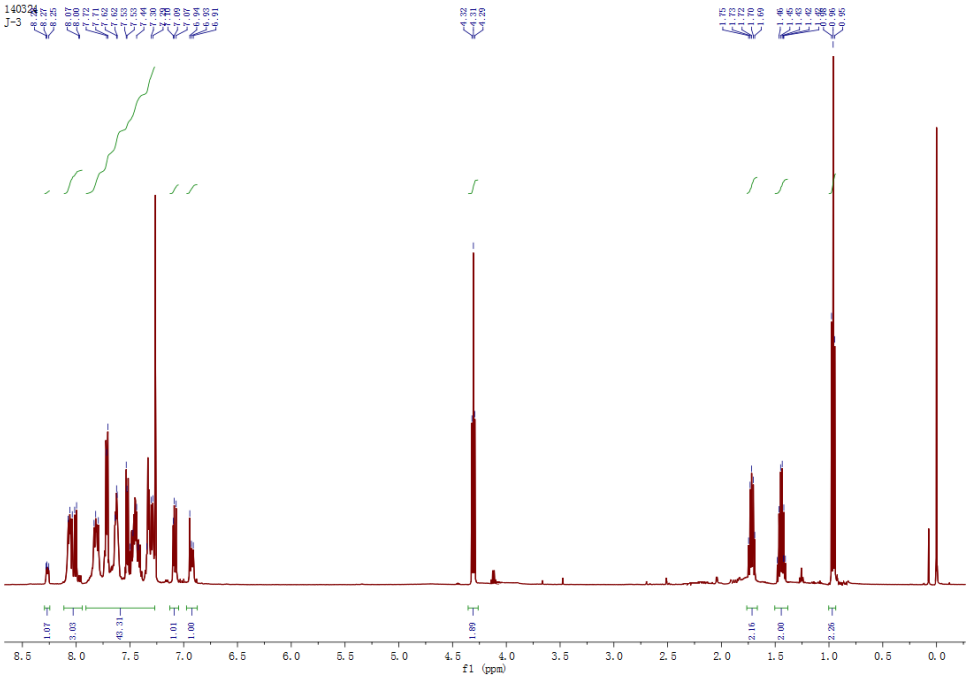

^{13}C NMR of **Mito-JN**

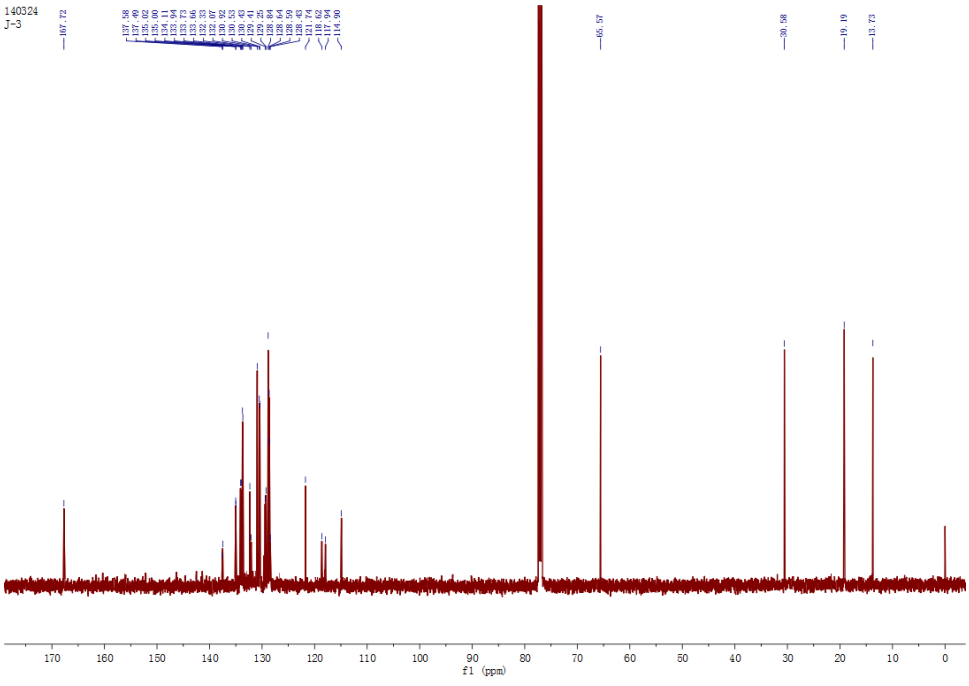

^{31}P NMR of **Mito-JN**

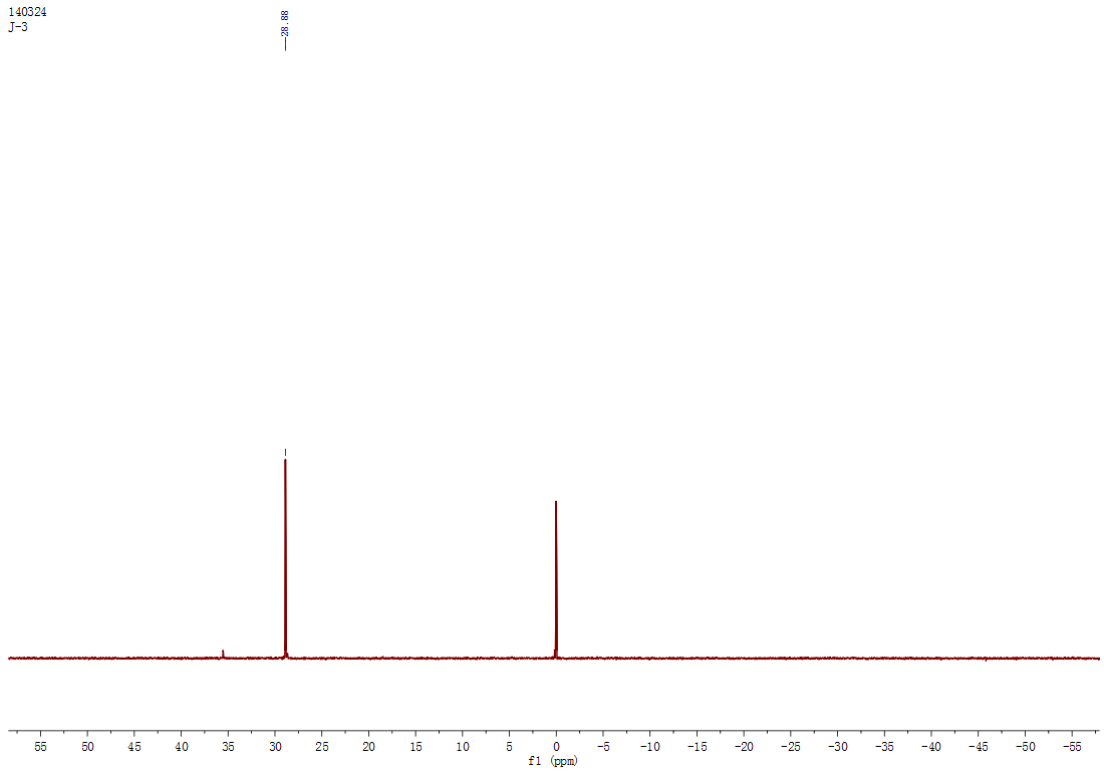

21. Reference

(1) S. B. King and H. T. Nagasawa, *Methods. Enzymol.*, **1999**, 301, 211-220.

(2) T. W. Hart, *Tetrahedron. Lett.*, **1985**, 26, 2013-2016.

(3) R. M. Uppu, *Anal. Biochem.*, **2006**, 354, 165-168.

(4) H. Maeda, K. Yamamoto, Y. Nomura, I. Kohno, L. Hafsi, N. Ueda, S. Yoshida, M. Fukuda, Y. Fukuyasu, Y. Yamauchi and N. Itoh, *J. Am. Chem. Soc.,* **2005**, 127, 68-69.

(5) (a) V. Massey and D. J. Edmondson, *Biol. Chem.*, **1970**, 245, 6595-6598; (b) D. Edmondson, V. Massey, G. Palmer, L. M. Beachan III and G. B. ELion, *J. Biol. Chem.*, **1972**, 247, 1597-1604.

(6) (a) J. A. Terao, A. Nagao, D. K. Park and B. P. Lim, *Meth. Enzymol.*, **1992**, 213, 454-460; (b) B. Chance, H. Sies and A. Boveris, *Proc. Natl. Acad. Sci. U.S.A.*, **1988**, 85, 3175-3179.

(7). T. Karstens and K. Kobs, J. Phys. Chem., 1980, 84, 1871.

(8). (a) A. Gorman, J. Killoran, C. O'Shea, T. Kenna, W. M. Gallagher and D. F. O'Shea, J. Am. Chem. Soc., 2004, 126, 10619-10631; (b) H. Stiel, K. Teuchner, A. Paul, W. Freyer and D. Leupold, J. Photochem. Photobiol. A., 1994, 80, 289-298.